Biointerface Research in Applied Chemistry
Open-Access Journal (ISSN: 2069-5837)

Article
Volume 15, Issue 5, 2025, 63
https://doi.org/10.33263/BRIAC155.063

In Silico Study of Bioactive Compound from Sungkai Leaves (*Peronema canescens Jack*) as Natural Inhibitor of 16-S rRNA

Muhammad Marsha Azzami Hasibuan [1], Dimas Andrianto [1], R. Haryo Bimo Setiarto [2,*]

[1] Department of Biochemistry, IPB University, Bogor, 16680, Indonesia; marshaazzami@apps.ipb.ac.id; (M.M.A.H.); dimasandrianto@apps.ipb.ac.id; (D.A.);
[2] Research Center for Applied Microbiology, National Research and Innovation Agency (BRIN), KST Soekarno, Cibinong, Bogor, 16911, Indonesia; (R.H.B.S.)
* Corresponding: rhar002@brin.go.id;

Received: 21.04.2025; Accepted: 24.07.2025; Published: 9.08.2025

Abstract: The rise of antibiotic-resistant bacteria has become a pressing global concern, leading to increased morbidity and mortality from infections that were once easily treatable. As these bacteria evolve and adapt, traditional methods of inhibition are becoming less effective, necessitating the development of innovative approaches to combat bacterial infections. One significant target of many antibiotics is the ribosomal RNA, specifically the 16S rRNA component of the bacterial ribosome, which inhibits protein synthesis. Every plant species is unique, as it can produce structurally different intermediates and metabolites, known as secondary metabolites, which protect against bacterial infections. The study is supplemented by considering reports of additional properties that may have potential applications in structure-activity relationships (SAR) research for the development of therapeutic drugs, as well as bioactivity radars related to the drug-like behaviour of the studied compounds. Based on the results of the sungkai (Peronema canescens Jack) bioavailability and toxicity test, followed by molecular docking against 16-S RNA, the test ligand SMR000036195 is considered safe, with a binding energy of 8.86 kcal/mol, compared to S-Adenosyl-D-homocysteine (8.47 kcal/mol). It can be concluded that SMR000036195 can serve as an alternative inhibitor of 16S rRNA, replacing S-adenosyl-L-homocysteine as a substrate for 16S rRNA inhibition.

Keywords: inhibitor; molecular docking; Sungkai; 16-S rRNA; YASARA.

1. Introduction

Bacteria are ubiquitous microorganisms that play essential roles in various ecosystems; however, certain pathogenic strains pose significant threats to human health. The rise in antibiotic-resistant bacteria has become a pressing global concern, leading to increased morbidity and mortality from infections that were once easily treatable. As these bacteria evolve and adapt, traditional methods of inhibition have become less effective, necessitating the development of innovative approaches to combat bacterial infections. Antimicrobial Resistance (AMR) occurs when bacteria evolve to resist the effects of medications that were once effective in treating them. The misuse and overuse of antibiotics, such as aminoglycosides, penicillin, and tetracycline, in humans, animals, and agriculture drive this

phenomenon. AMR is recognized as one of the top global public health threats, directly responsible for approximately 1.27 million deaths annually, with a contribution to nearly 5 million deaths globally in 2019 [1]. The WHO has emphasized that AMR affects all regions and income levels, but low- and middle-income countries are particularly vulnerable due to inadequate healthcare resources.

Antibiotics play a crucial role in inhibiting bacterial growth and survival, particularly by affecting essential cellular processes. One significant target of many antibiotics is ribosomal RNA, specifically the 16S rRNA component of the bacterial ribosome. One of the methods used by antibiotics targeting 16S rRNA is the inhibition of protein synthesis. Antibiotics, such as aminoglycosides and tetracyclines, bind to the 16S rRNA within the 30S ribosomal subunit. This binding disrupts the decoding process during protein synthesis, leading to misreading of mRNA and production of faulty proteins, which can ultimately kill or inhibit bacterial growth [2].

The development of new antibiotics faces numerous challenges that hinder progress and innovation in combating antibiotic resistance. Several of the challenges from scientific points are: high failure rate (only about one in 15 drugs make it to patients, and for new classes, this drops to one in 30) and lack of novelty (since the 1980s, no new classes of antibiotics have been discovered, leading to a reliance on modifications of existing drugs, increasing vulnerability of new drugs to cross-resistance with existing treatments). Economic challenges include high development cost, long testing phase (developing a new antibiotic can take 10-15 years and cost over $1 billion), and regulatory complexity (the regulatory pathways for antibiotic approval can be lengthy and complicated). This can slow the process of bringing new antibiotics to the market [3].

Plants have existed in the universe for over 400 million years and possess unique characteristics that enable them to protect themselves from infections. Every plant species is unique because it can produce structurally distinct intermediates and metabolites, known as secondary metabolites. A wide variety of secondary metabolites, including tannins, terpenoids, alkaloids, and flavonoids, which are abundantly found in plants, have been reported to possess antimicrobial properties. The vast chemical diversity provided by plant-derived compounds may contribute to the antimicrobial mechanisms of secondary metabolites, which may enable them to be considered as potential targets [4].

To overcome this challenge, the development of alternative treatments for bacterial infections is emerging, particularly through approaches that target plant secondary metabolites. These natural compounds, produced by plants as part of their defense mechanism, have shown promising antibacterial properties. This research is complemented by considering reports on several additional properties of potential applications in structure-activity relations (SAR) studies for therapeutic drug development, as well as with a bioactivity radar related to the drug-like behavior of the studied compounds, predicted biochemical targets, and values associated with pharmacokinetics and ADMET properties through standard chemoinformatics procedures [5–11]. Current research represents studies on the properties of some families of therapeutic compounds of Sungkai origin.

2. Materials and Methods

2.1. Materials.

This research was conducted using a computer device with a Windows 11 Professional 64-bit operating system, an x64-based processor, and an AMD Ryzen 5 5600 H processor with a base clock speed of 3.30 GHz and a maximum turbo frequency of 4.20 GHz. The software used was Yet Another Scientific Artificial Reality Application (YASARA) structure, BIOVIA Discovery Studio 2024, and ChimeraX. All test ligand materials were downloaded from PubChem (https://pubchem.ncbi.nlm.nih.gov), and receptors from RCSB PDB (https://www.rcsb.org).

2.2. Methods.

2.2.1. Protein functional sites.

Research on the functional sites of the identified protein was done using CD-search on the CDD webserver11 (ncbi.nlm.nih.gov/Structure/cdd/wrpsb.cgi) [9] and Computed Atlas of Surface Topography of the universe of protein Folds (CASTpFold) webserver https://cfold.bme.uic.edu/castpfold/ [11].

2.2.2. Pharmacokinetic test.

The molecular structures of the bioactive compound from Peronema canescens Jack were obtained from PubChem. One of the most crucial pieces of information to gather before beginning research on the identification and creation of novel therapeutic therapies is pharmacokinetics. Typically, this is accomplished using separate indicators known as ADMET (absorption, distribution, metabolism, excretion, and toxicity) factors. Using online SwissADME software, various ADME parameters were computed for this study (swissadme.ch) [8,12]. By using pkCSM (biosig.lab.uq.edu.au/pkcsm/prediction) and Deep-PK (biosig.lab.uq.edu.au/deeppk/), additional information related to the ADMET properties and the pharmacokinetics parameters was identified [10,12].

2.2.3. Toxicity prediction.

Toxicity predictions were conducted for these compounds to assess their safety for human use. The analysis utilized ProTox-III (tox.charite.de/protox3), an online tool designed to predict the toxicity of small molecules. The compounds were submitted to the server, which generated toxicity profiles and enabled comparisons with known drugs such as Atorvastatin and Orlistat [7].

2.2.4. Ligands and receptor preparation.

The test ligands were obtained from the PubChem database. The 3P2E protein was chosen as the target receptor and imported into the Yasara Structure software. The protein structure was prepared by adding a hydrogen atom, removing the water molecule, and deleting any unused ligands. The test compounds were then optimized by minimizing their binding energy using the "Energy minimization" experiment in the YASARA Structure program. Both receptor and ligand were saved in a *.pdb file format [13].

2.2.5. Molecular docking between ligands and receptor.

The receptor was docked with ligands using YASARA. Redocking was performed to determine the most suitable Grid box size. This process was then continued for screening. YASARA structure with the dock_run.mcr.macro script was executed with 100 runs, and the Amber14 force field was used for validation [14]. The dock_runscreening macro file, written by Elmar Krieger for the YASARA structure, is used to attach an unlimited number of ligands to the target receptor using the VINA or AutoDock methods. The resulting binding energy values are then sorted accordingly (yasara.org/dock_runscreening.mcr). Screening utilises the YASARA structure with the macrodock_runscreening macro.mcr set in the VINA method, runs=100, and Amber14 [13].

2.2.6. Data analysis.

BIOVIA Discovery Studio 2024 and ChimeraX version 1.8 software were used to analyse and visualise the screening data in two and three dimensions. Using the YASARA structure, the (.yob) files or objects containing complexes are transformed into (.pdb) format for simpler 2D and 3D visualization with BIOVIA Discovery Studio and ChimeraX [14].

3. Results and Discussion

The test ligands used in this research were 42 active compound ligands of Peronema canescens Jack and one comparison ligand, S-adenosyl-D-homocysteine (SAH) [15]. The first physicochemical test performed was the Lipinski Rules of Five. Four ligands were eliminated from the 43 ligands that were tested. ADMET parameters, including intestinal absorption, AMES toxicity, hERG blockers, carcinogenesis, and LD_{50}, were applied to test the remaining 39 ligands. Thirteen of the 39 ligands evaluated were eliminated, while the remaining ligands proceeded to the next phase of evaluation. Five compounds with the best Gibbs free energy values were selected through virtual screening of 26 test ligands. After docking the five ligands with the receptor, the results were compared with those obtained for SAH. Based on the interaction between the ligand and receptor, the best ligands were visualized and compared with SAH.

3.1. Pharmacokinetic test.

The Lipinski Rules of five (Table 1) pharmacokinetic criteria are used when studying substances that resemble very important drugs. Molecular weight, log p, rotatable bonds, donors and acceptors, and surface area are criteria of the Lipinski Rules of 5. If a compound fails to meet one or more of these criteria, it is predicted to have bioavailability problems. Utilizing established criteria, Lipinski's rule explains the physicochemical characteristics of each compound [10]. Out of the 43 ligands tested, four ligands were eliminated. The bioavailability radars of the top five ligands that passed the bioavailability test and SAH are shown in Figure 1.

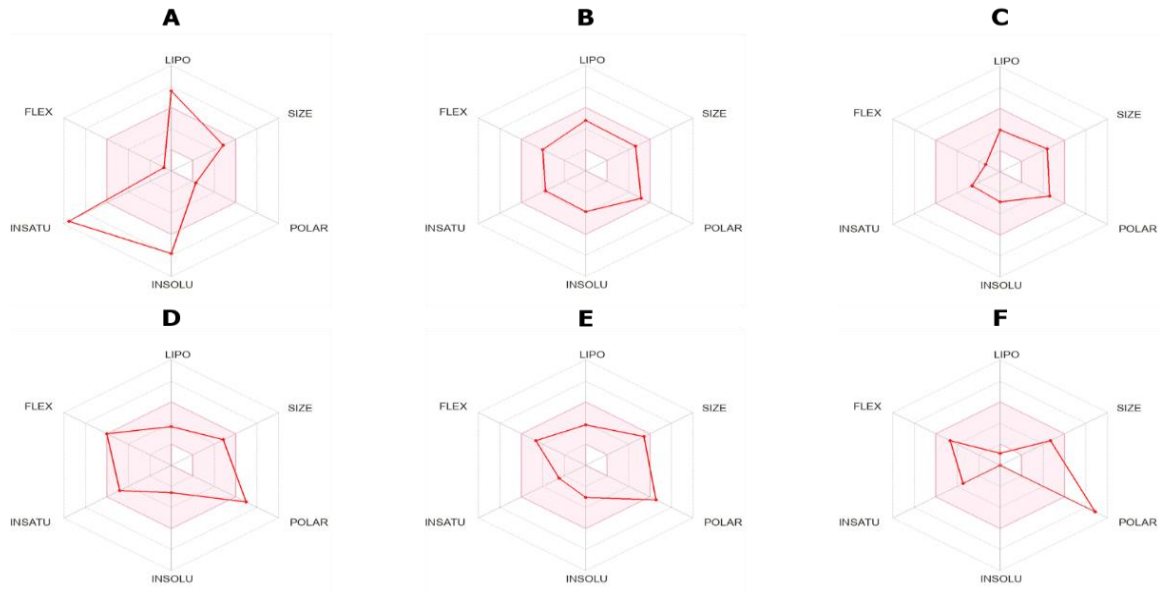

Figure 1. The bioavailability radars of S-Adenosyl-D-homocysteine (SAH) test ligands **(A)** DTXSID50454478; **(B)** SMR000036195; **(C)** Prednisone; **(D)** MLS001002312; **(E)** CHEMBL2346880; **(F)** SAH.

Table 1. Results of Lipinski's rules of the 5 bioavailability test.

Ligand	Lipinski's Rules of 5					
	MW	**Log P**	**RB**	**H_A**	**H_D**	**TPSA**
Acceptable Value	≤ 500	≤ 5	≤ 10	≤ 10	≤ 5	≤ 140
DTXSID50454478	398.52	7.76	1.00	0.00	0.00	28.24
SMR000036195	382.43	3.11	6.00	7.00	0.00	107.20
Prednisone	358.43	1.77	2.00	5.00	2.00	91.67
MLS001002312	398.50	1.62	9.00	6.00	2.00	156.89
CHEMBL2346880	450.96	1.29	7.00	7.00	1.00	145.53
S-Adenosyl-D-homocystein	384.41	-1.75	7.00	9.00	5.00	207.93

The red value indicates failure to fulfill Lipinski Ro5 test parameters.

The remaining 39 ligands were evaluated using ADMET parameters, including intestinal absorption, Ames toxicity, hERG Blockers, Carcinogenesis, and LD50 (Table 2). Out of the 39 ligands tested, 13 ligands were eliminated, and the rest advanced to the next test stage. Virtual screening revealed that among the 26 test ligands, five compounds exhibited the most favourable Gibbs free energy values. The five ligands were then docked with the receptor, and the results were compared with the avibactam docking result. Table 2 describes the result of several criteria selected from ADMET, consisting of Intestinal Absorption (>30% to be in the safe category), AMES Toxicity ("safe" result to enter the safe category), Human Ether-A-Go-Go Related Gene (hERG) blocker ("safe" result to enter the safe category) carcinogenesis ("Safe" result to enter the safe category), and LD_{50} (>300 mg/KgBW/day to enter the safe category) [7,10].

Table 2. Results of ADMET test.

Ligand	ADMET				
	Intestinal absorption	**AMES toxicity**	**hERG blockers**	**Hepatotoxicity**	**LD_{50}**
Acceptable Value	>0.3	Safe	Safe	Safe	≥300 mg/kg
DTXSID50454478	1.00	Toxic	Safe	Toxic	1000 mg/kg, Class 4
SMR000036195	0.98	Safe	Safe	Safe	2730 mg/kg, Class 5
Prednisone	1.00	Toxic	Safe	Toxic	1680 mg/kg, Class 4
MLS001002312	0.91	Safe	Safe	Safe	1000 mg/kg, Class 4
CHEMBL2346880	0.95	Safe	Safe	Safe	250 mg/kg, Class 3
S-Adenosyl-D-homocystein	0.36	Toxic	Safe	Safe	3320 mg/kg, Class 5

The red value indicates failure to fulfill one/more of the ADMET test parameters.

Lipinski's criteria can be used for pharmacokinetic screening. These say that the molecules that are most "drug-like" should have a Log P value of ≤ 5, a molecular weight of ≤ 500, no more than 10 hydrogen bond acceptors, no more than 5 hydrogen bond donors, and a topological polar surface area (TPSA) of ≤ 140 Å^2. Molecules that do not meet one or more of these criteria may exhibit bioavailability issues [16]. This rule is known as the rule of 5. Having no more than 10 rotatable bonds and a maximum of 10 hydrogen bond donors and five hydrogen bond acceptors are the fifth and sixth requirements, respectively. In the human body, drug absorption begins in the intestinal epithelium, travels through the bloodstream, and ultimately reaches the site of action of the drug. Compounds weighing more than 500 Daltons have been shown in earlier research to have less-than-ideal absorption properties [16]. According to Table 1, all the tested ligands met these criteria successfully.

The acceptable range for lipophilicity is Log P ≤ 5, according to the second criterion, Log P. Drug candidates that surpass this limit often demonstrate reduced solubility in physiological fluids, preventing them from reaching the membrane surface. Overly hydrophilic compounds may struggle to cross cell membranes and reach their intended target sites. In contrast, excessively hydrophobic compounds (Log P > 5) tend to stay at the first membrane they come into contact with [16]. According to Table 1, DTXSID50454478 failed the Log P test. Any single non-ring bond attached to a non-terminal heavy atom (i.e., a non-hydrogen atom) is referred to as a rotatable bond. Because amide C-N bonds have a large rotational energy barrier, they were excluded from this formulation. This simple topological metric has been shown to be a good predictor of oral medication bioavailability and an indicator of molecular flexibility [16]. As shown in Table 1, all of the test ligands passed this test.

Drug efficacy is directly influenced by the physicochemical characteristics of a molecule, such as solubility, absorption, and distribution, which are also significantly affected by the number of hydrogen bond donors and acceptors. It is recommended that there should be fewer than five hydrogen bond donors and fewer than ten acceptors for the best absorption and permeability. A compound may be too polar to cross cell membranes if it diverges efficiently from this rule [16]. As shown in Table 1, all ligands passed the hydrogen donor and acceptor tests. The topological polar surface area (TPSA) of pharmacological molecules directly affects their absorption by biological membranes, including those found in the brain and central nervous system nerve cells. Drugs with a dynamic TPSA of less than 60 Å^2 are completely absorbed, whereas those with a TPSA of more than 140 Å^2 have limited permeability [17]. As shown in Table 1, MLS001002312, CHEMBL2346880, and SAH failed the TPSA test.

Absorption, Distribution, Metabolism, Excretion, and Toxicity (ADMET) is a crucial component in assessing the pharmacokinetic and pharmacodynamic properties of pharmaceutical compounds. Optimising novel drug possibilities involves calculating ADMET properties. Successful drug development requires favourable ADMET characteristics and excellent therapeutic action. Understanding how medications are absorbed, particularly when administered orally, and how they are absorbed into the digestive system, is an important aspect of drug research. Poor absorption can lead to neurotoxicity and nephrotoxicity, which can negatively impact circulation and metabolism. Therefore, the purpose of this study is to elucidate the function of drug molecules within an organism. Consequently, examining ADMET properties is an essential aspect of computational drug design [12].

When a chemical enters the bloodstream, it can reach the tissue. Medicines are often delivered through mucous surfaces, such as the digestive tract, before being absorbed by the target cells. Poor substance solubility, intestinal transit time, gastric emptying time, difficulty

in permeating the intestinal wall, and chemical instability in the stomach are all factors that contribute to reduced drug absorption following oral delivery. Drugs with low absorption are less acceptable for oral delivery, such as inhalation or intravenous [10,12]. A molecule with an Intestinal Absorption of less than 30% is considered poorly absorbed. Based on Table 2, all tested ligands met these criteria successfully.

AMES toxicity testing is a standard approach for determining the mutagenic potential of a drug using bacterial assays. A positive result from this test indicates that the substance under investigation may be mutagenic and act as a carcinogen [6,7,10]. Based on Table 2, prednisone, DTXSID50454478, and CHEMBL2346880 failed this test. The criteria for hERG inhibitors indicate that the blockage of potassium channels encoded by hERG (human ether-a-go-go gene) is a key factor in the development of QT syndrome, which can lead to serious ventricular arrhythmias in the heart [10]. Based on Table 2, all the tested ligands met these criteria successfully. Drug-induced liver injury is a significant safety issue in drug development and a major reason for the failure of drugs in the market. A compound is classified as hepatotoxic if it is associated with at least one pathological or physiological liver event that is closely associated with impaired liver function. As shown in Table 2, prednisone and DTXSID50454478 failed the test.

The toxicity of potential compounds is very important. The lethal dosage value (LD_{50}) is a standard measure of acute toxicity to assess toxicity relative to other molecules. LD_{50} is the amount of compound administered directly that is capable of causing the death of 50% of the test animals. In ProTox-III, there are six classes, ranging from non-harmful to fatal, in which class 1 has an $LD_{50} \leq 5$, which is fatal if consumed, up to class 6 with an $LD_{50} > 5000$, indicating that the compound is non-toxic [6,7]. As shown in Table 2, all of the test ligands passed this test.

3.2. Molecular docking between ligands and receptor.

The grid box size used for the screening was 3 Å, as this size yielded an RMSD value of 0.13 and a binding energy of 8.86 kcal/mol upon redocking. This research provides screening results in the form of binding energy, residual contact, and types of interactions formed. The 16S rRNA (PDB: 3P2E) does not have any conserved functional sites predicted by the Conserved Domain Database (CDD) server [9]. CASTpFOLD results showed that residues GLY 32, ASN 38, ASP 55, ALA 87, GLU 88, LEU 104 – THR 109, and ALA 195 – TRP 197 act as the binding site residues [11,18]. Table 3 shows the ranking of the top five ligands based on their binding energies. A positive score indicates the best binding energy in the YASARA structure. Thus, a score with a more positive result indicates better binding of the ligand to the receptor [14]. Receptor interactions with SAH are shown in Figure 2, whereas those with SMR000036195 are shown in Figure 3.

Table 3. Sungkai molecular docking results with 16-S rRNA receptor.

Ligand	Effi [kcal/(mol*Atom)]	Bind.energy [kcal/mol]	Dissoc. constant[pM]
DTXSID50454478	0.31	9.30	1.52E+05
SMR000036195	0.33	8.47	6.18E+05
Prednisone	0.31	8.00	1.36E+06
MLS001002312	0.30	7.87	1.69E+06
CHEMBL2346880	0.28	7.83	1.82E+06
S-Adenosyl-D-homocystein	0.34	8.86	3.21E+05

The red ligand violates one/more of the pharmacokinetic test parameters.

S-adenosyl-D-homocysteine (SAH) was used as a binding energy control so that the test ligand that has a binding energy above SAH can be considered as a potential ligand to be developed. Based on Table 3, the ligand used as a control (CID_439155) has a binding energy of 8.86 kcal/mol. The test ligands with binding energy above SAH are DTXSID50454478 (9.30 kcal/mol), while ligands with binding energy below SAH are SMR000036195 (8.47 kcal/mol), prednisone (8.00 kcal/mol), MLS001002312 (7.87 kcal/mol), and CHEMBL2346880 (7.83 kcal/mol). By sorting the best receptor-ligand complex, the YASARA structure identifies the one with the highest score. Therefore, a score with a more positive result indicates better binding of the ligand to the receptor [13].

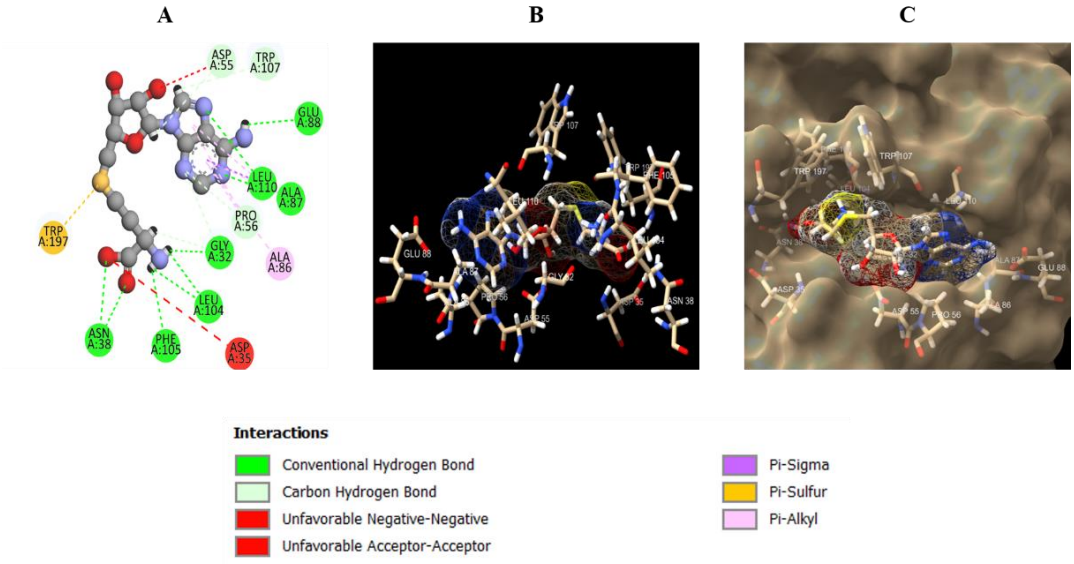

Figure 2. SAH interaction with 16-S rRNA receptor visualized in 2D and 3D**.**

In addition, a small Kd value indicates stronger ligand binding to the receptor [13,19]. The ligand efficiencies of SMR000036195 were 0.34, while that of avibactam was 0.41, indicating that the binding energy contributed per atom of the compounds was close enough to the required energy to develop key contacts with the 16-S rRNA receptor target [13,20]. The range of ligand efficiency under S-adenosyl-D-homocysteine (based on binding energy) was 0.28 to 0.34. Based on the results from Lipinski Ro5 and ADMET, followed by molecular docking with the 16S rRNA receptor, we selected SMR000036195 as the best test ligand to serve as a candidate alternative inhibitor.

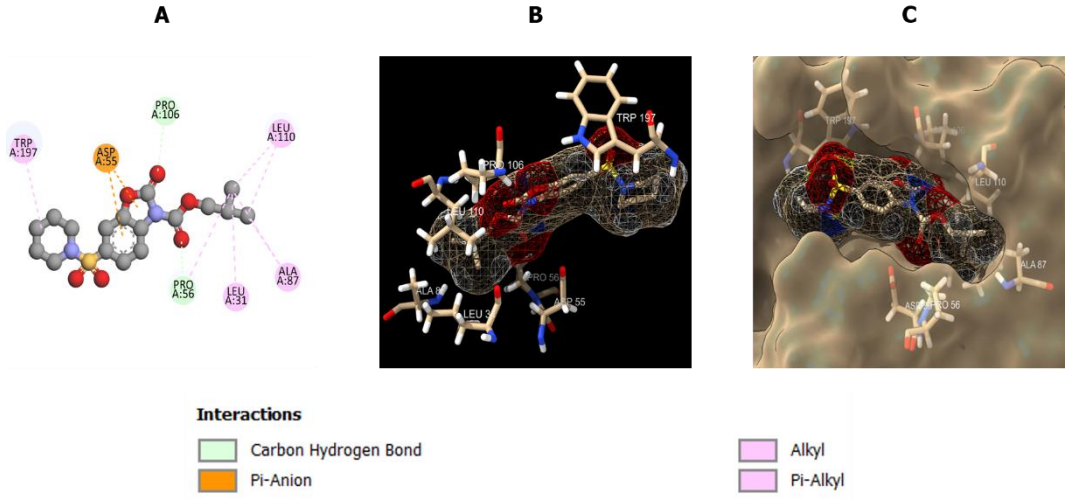

Figure 3. SMR000036195 interaction with 16-S rRNA receptor visualized in 2D and 3D.

Table 4 shows the interactions that occurred between each test ligand, categorising them into two main categories: hydrogen bonds and hydrophobic interactions. Hypothetically, the more hydrogen bonds the ligand has, the easier and stronger it binds to the active side of the receptor. A good hydrogen bond has a distance of less than 2.3 Å. Hydrophobic bonds are considered important due to their role in stabilising the interaction between ligands and receptors [21,22]. As shown in Table 4, nearly all the formed interaction bonds occurred in the active and/or binding sites.

Table 4. Residue interaction analysis between test ligands and 16-S rRNA receptor.

Ligand	Residues/amino acids involved	
	Hydrophobic interaction	**Hydrogen bond**
DTXSID50454478	A VAL 57, **A LEU 196**, **A TRP 197**	-
SMR000036195	A LEU 31, A PRO 56, **A ALA 87**, A LEU 110, **A TRP 197**	A PRO 56, **A PRO 106**
Prednisone	**A TRP 197**	A ARG 200
MLS001002312	A PRO 56, **A LEU 104**, A LEU 110	A ASP 30, **A GLY 32**, A THR 33, A GLY 34, **A ASN 38**, **A LEU 104**, **A THR 109**, A LEU 110
CHEMBL2346880	**A LEU 104**, **A PHE 105**, **A TRP 107**, **A TRP 197**	A GLY 34, **A ASP 55**
S-Adenosyl-D-homocystein	A PRO 56, A ALA 86, **A ALA 87**, A LEU 110	**A GLY 32**, **A ASN 38**, **A ASP 55**, A PRO 56, **A ALA 87**, **A GLU 88**, **A LEU 104**, **A PHE 105**, **A TRP 107**, A LEU 110

Amino acids in bold indicate the presence of contact with the active site and/or binding site.

SAH (S-Adenosyl-D-homocysteine) is the ligand that acts as a substrate standard for this study [15]. S-adenosyl-D-homocysteine forms both hydrogen bonds and hydrophobic interactions. The hydrogen bonds formed consist of conventional hydrogen bonds and carbon-hydrogen bonds. Conventional hydrogen bonds were formed between the ligand and amino acid residues GLY 32 (2.74 A), ASN 38 (2.42 and 2.86 A), ALA 87 (2.00 A), GLU 88 (2.45 A), LEU 104 (2.28 and 2.54 A), PHE 105 (2.54 A), and LEU 110 (2.56 A) (Table 4). Carbon-hydrogen bonds were formed between the ligand and amino acid residues GLY 32 (2.45 and 2.85 A), ASP 55 (2.80 A), PRO 56 (3.06 A), and TRP 107 (3.05 A). The hydrophobic bonds consist of Pi-sigma and Pi-alkyl bonds. Pi-sigma bond formed between the ligand and amino acid residue of LEU 110 (2.87 A), while pi-alkyl bonds formed between the ligand and amino acid residues PRO 56 (4.63 and 5.05 A), ALA 86 (4.92 A), ALA 87 (4.63 A), and LEU 110 (4.29 A). SMR000036195 (Figure 3) formed both hydrogen and hydrophobic bonds. The hydrogen bonds formed were carbon-hydrogen bonds, which occurred in PRO 56 (2.65 A) and PRO 106 (2.65 A). Hydrophobic interactions consist of alkyl and π-alkyl bonds. Alkyl bonds occurred with residues LEU 31 (4.86 A), PRO 56 (4.55 A), ALA 87 (3.87 and 4.45 A), and LEU 110 (4.04 and 4.06 A). π-alkyl bonds occurred with residue TRP 197 (5.48 A).

4. Conclusions

Based on the results of the sungkai (*Peronema canescens Jack*) bioavailability and toxicity tests, followed by molecular docking against 16S rRNA, the test ligand SMR000036195 was considered safe. Its binding energy was close to that of homocysteine (8.86 kcal/mol vs. 8.47 kcal/mol). It can be concluded that SMR000036195 may serve as an alternative inhibitor of 16S rRNA, potentially replacing homocysteine as a substrate for 16S rRNA inhibition. This result must be validated by further experimentation, such as Molecular Dynamics, in Vitro, and in Vivo testing.

Author Contributions

Conceptualization, M.M.A.H. and R.H.B.S.; methodology, M.M.A.H., D.A., and R.H.B.S.; software, M.M.A.H.; validation, D.A. and R.H.B.S.; formal analysis, M.M.A.H.; investigation, D.A. and R.H.B.S.; resources, M.M.A.H., D.A., and R.H.B.S.; data curation, M.M.A.H.; writing—original draft preparation, M.M.A.H., D.A., and R.H.B.S.; writing—review and editing, M.M.A.H., D.A., and R.H.B.S.; visualization, M.M.A.H.; supervision, D.A. and R.H.B.S.; project administration, D.A. and R.H.B.S. All authors have read and agreed to the published version of the manuscript.

Institutional Review Board Statement

Not applicable.

Informed Consent Statement

Not applicable.

Data Availability Statement

Data supporting the findings of this study are available upon reasonable request from the corresponding author.

Funding

This research received no external funding.

Acknowledgments

The author would like to thank all parties who have contributed to the completion of this research. All authors made equal contributions as the main contributors to this manuscript.

Conflicts of Interest

The authors declare that they have no conflict of interest.

References

1. Iredell, J. Antimicrobial resistance. *Microbiol. Aust.* **2019**, *40*, 55–56.
2. Kapoor, G.; Saiga, S.; Elongavan, A. Action and resistance mechanisms of antibiotics: A guide for clinicians. *J. Anaesthesiol. Clin. Pharmacol*. **2017**, *33*, 300-305, https://doi.org/10.4103/joacp.JOACP_349_15.
3. Anderson, M.; Panteli, D.; van Kessel, R.; Ljungqvist, G.; Colombo, F.; Mossialos, E. Challenges and opportunities for incentivising antibiotic research and development in Europe. *Lancet Reg. Health - Eur.* **2023**, *33*, 100705, https://doi.org/10.1016/j.lanepe.2023.100705.
4. Arip, M.; Selvaraja, M.; Mogana, R.; Tan, L.F.; Leong, M.Y.; Tan, P.L.; Yap, V.L.; Chinnapan, S.; Tat, N.C.; Abdullah, M.; Dharmendra, K.; Jubair, N. Review on Plant-Based Management in Combating Antimicrobial Resistance - Mechanistic Perspective. *Front. Pharmacol*. **2022**, *13*, 879495, https://doi.org/10.3389/fphar.2022.879495.
5. Alazmi, M.; Motwalli, O. In silico virtual screening, characterization, docking and molecular dynamics studies of crucial SARS-CoV-2 proteins. *J. Biomol. Struct. Dyn*. **2021**, *39*, 6761–6771, https://doi.org/10.1080/07391102.2020.1803965.
6. Banerjee, P.; Dehnbostel, F.O.; Preissner, R. Prediction is a balancing act: Importance of sampling methods to balance sensitivity and specificity of predictive models based on imbalanced chemical data sets. *Front. Chem*. **2018**, *6*, 362, https://doi.org/10.3389/fchem.2018.00362.

7. Banerjee, P.; Kemmler, E.; Dunkel, M.; Preissner, R. ProTox 3.0: A webserver for the prediction of toxicity of chemicals. *Nucleic Acids Res*. **2024**, *52*, W513–20, https://doi.org/10.1093/nar/gkae303.
8. Daina, A.; Michielin, O.; Zoete, V. SwissADME: A free web tool to evaluate pharmacokinetics, drug-likeness and medicinal chemistry friendliness of small molecules. *Sci. Rep*. **2017**, *7*, 42717, https://doi.org/10.1038/srep42717.
9. Marchler-Bauer, A.; Bo, Y.; Han, L.; He, J.; Lanczycki, C.J.; Lu, S.; Chitsaz, F.; Derbyshire, M.K.; Geer, R. C.; Gonzales, N. R.; Gwadz, M.; Hurwitz, D.I.; Lu, F.; Marchler, G.H.; Song, J.S.; Thanki, N.; Wang, Z.; Yamashita, R. A.; Zhang, D.; Zheng, C.; Geer, L.Y.; Bryant, S.H. CDD/SPARCLE: Functional classification of proteins via subfamily domain architectures. *Nucleic Acids Res*. **2017**, *45*, D200–D203, https://doi.org/10.1093/nar/gkw1129.
10. Pires, D.E.V.; Blundell, T.L.; Ascher, D.B. pkCSM: Predicting small-molecule pharmacokinetic and toxicity properties using graph-based signatures. *J. Med. Chem*. **2015**, *58*, 4066–4072, https://doi.org/10.1021/acs.jmedchem.5b00104.
11. Ye, B.; Tian, W.; Wang, B.; Liang, J. CASTpFold: Computed Atlas of Surface Topography of the universe of protein Folds. *Nucleic Acids Res*. **2024**, *52*, W194–W199, https://doi.org/10.1093/nar/gkae415.
12. Flores-Holguín, N.; Frau, J.; Glossman-Mitnik, D. In Silico Pharmacokinetics, ADMET Study and Conceptual DFT Analysis of Two Plant Cyclopeptides Isolated From Rosaceae as a Computational Peptidology Approach. *Front. Chem*. **2021**, *9*, 708364, https://doi.org/10.3389/fchem.2021.708364.
13. Gholam, G.M.; Mahendra, F.R.; Irsal, R.A.P.; Dwicesaria, M.A.; Ariefin, M.; Kristiadi, M.; Rizki, A.F.M.; Azmi, W.A.; Artika, I.M.; Siregar, J.E. Computational Exploration of Compounds in Xylocarpus granatum as a Potential Inhibitor of Plasmodium berghei Using Docking, Molecular Dynamics, and DFT Studies. *Biochem. Biophys. Res. Commun*. **2024**, *733*, 150684, https://doi.org/10.1016/j.bbrc.2024.150684.
14. Irsal, R.A.P.; Gholam, G.M.; Dwicesaria, M.A.; Chairunisa, F. Computational investigation of Y. aloifolia variegate as anti-Human Immunodeficiency Virus (HIV) targeting HIV-1 protease: A multiscale in-silico exploration. *Pharmacol. Res. - Mod. Chinese Med*. **2024**, *11*, 100451, https://doi.org/10.1016/j.prmcm.2024.100451.
15. Husain, N.; Obranić, S.; Koscinski, L.; Seetharaman, J.; Babić, F.; Bujnicki, J.M.; Maravić-Vlahoviek, G.; Sivaraman, J. Structural basis for the methylation of A1408 in 16S rRNA by a panaminoglycoside resistance methyltransferase NpmA from a clinical isolate and analysis of the NpmA interactions with the 30S ribosomal subunit. *Nucleic Acids Res*. **2011**, *39*, 1903–1918, https://doi.org/10.1093/nar/gkq1033.
16. Sahu, V.K.; Singh, R.K.; Singh, P.P. Extended Rule of Five and Prediction of Biological Activity of peptidic HIV-1-PR Inhibitors. *Trends J. Sci. Res.* **2022**, *1*, 20–42. https://doi.org/10.31586/ujpp.2022.403.
17. Karami, T.K.; Hailu, S.; Feng, S.; Graham, R.; Gukasyan, H.J. Eyes on Lipinski's Rule of Five: A New "Rule of Thumb" for Physicochemical Design Space of Ophthalmic Drugs. *J. Ocul. Pharmacol. Ther.* **2022**, *38*, 43–55, https://doi.org/10.1089/jop.2021.0069.
18. Ji, Z.; Kozuch, J.; Mathews, I.I.; Diercks, C.S.; Shamsudin, Y.; Schulz, M.A.; Boxer, S.G. Protein Electric Fields Enable Faster and Longer-Lasting Covalent Inhibition of β-Lactamases. *J. Am. Chem. Soc*. **2022**, *144*, 20947–20954, https://doi.org/10.1021/jacs.2c09876.
19. Aamir, M.; Singh, V.K.; Dubey, M.K.; Meena, M.; Kashyap, S.P.; Katari, S.K.; Upadhyay, R.S.; Umamaheswari, A.; Singh, S. In silico prediction, characterization, molecular docking, and dynamic studies on fungal SDRs as novel targets for searching potential fungicides against fusarium wilt in tomato. *Front. Pharmacol.* **2018**, *9*, 1038, https://doi.org/10.3389/fphar.2018.01038.
20. Patel, C.N.; Goswami, D.; Jaiswal, D.G.; Parmar, R.M.; Solanki, H.A.; Pandya, H.A. Pinpointing the potential hits for hindering interaction of SARS-CoV-2 S-protein with ACE2 from the pool of antiviral phytochemicals utilizing molecular docking and molecular dynamics (MD) simulations. *J. Mol. Graph. Model.* **2021**, *105*, 107874, https://doi.org/10.1016/j.jmgm.2021.107874.
21. Uzzaman, M.; Hasan, M.K.; Mahmud, S.; Yousuf, A.; Islam, S.; Uddin, M.N.; Barua, A. Physicochemical, spectral, molecular docking and ADMET studies of Bisphenol analogues; A computational approach. *Informatics Med. Unlocked*. **2021**, *25*, 100706, https://doi.org/10.1016/j.imu.2021.100706.
22. Irsal, R.A.P.; Hami Seno, D.S.; Safithri, M.; Kurniasih, R. Penapisan Virtual Senyawa Aktif Sirih Merah (Piper crocatum) sebagai Inhibitor Angiotensin Converting Enzyme. *J. Farmamedika* **2022**, *7*, 104–113, https://doi.org/10.47219/ath.v7i2.157.

Publisher's Note & Disclaimer

information before relying on it, and the publisher assumes no responsibility for any consequences arising from the use of materials contained in this publication.